THE LHC VACUUM SYSTEM

O. Gröbner, CERN, 1211 Geneva 23, Switzerland

Abstract

The Large Hadron Collider (LHC) at CERN, involves two proton storage rings with colliding beams of 7 TeV. The machine will be housed in the existing LEP tunnel and requires 16 m long superconducting bending magnets. The vacuum chamber will be the inner wall of the cryostat and hence at the temperature of the magnet cold bore, i.e. at 1.9 K and therefore a very good cryopump. To reduce the cryogenic power consumption, the heat load from synchrotron radiation and from the image currents in the vacuum chamber will be absorbed on a 'beam screen', which operates between 5 and 20 K, inserted in the magnet cold bore. The design pressure necessary for operation must provide a lifetime of several days and a further stringent requirement comes from the power deposition in the superconducting magnet coils due to protons scattered on the residual gas which could lead to a magnet quench. Cryopumping of gas on the cold surfaces provides the necessary low gas densities but it must be ensured that the vapour pressure of cryosorbed molecules, of which H_2 and He would be the most critical species, remains within acceptable limits. In the room temperature sections of the LHC, specifically in the experiments, the vacuum must be stable against ion induced desorption and ISR-type 'pressure bumps'.

1 INTRODUCTION

The Large Hadron Collider (LHC) [1] will be installed in the existing 27 km underground tunnel of the Large Electron Positron collider (LEP) at CERN in Geneva. The main element of the new accelerator/storage ring will be a string of superconducting magnets, dipoles and quadrupoles, which bend and focus the two counter rotating proton beams with a design energy of 7 TeV. The bending radius is 2784 m and the magnetic field will be 8.3 T. The dipole magnets are mounted in a 'two-in-one' configuration within the same cold iron yoke and in the same common cryostat. The two inner tubes of this cryostat, in direct contact with the 1.9 K helium, fulfil the function of the vacuum chamber for the machine. With this design, the LHC will be the first high energy storage ring with a vacuum system at cryogenic temperature which is exposed to intense synchrotron radiation emitted from proton beams. The design intensity of each beam is 0.53 A (but only about 0.053 A during the first period of operation). Due to the very high energy of the proton beams and since the 'cold-bore' beam pipe is a very effective cryopump, a number of novel design requirements as well as constraints will have to be met. The general design of the vacuum system for LHC [2, 3, 4] has been presented at several conferences and, therefore, only the most important characteristics and the results from some recent studies will be described here. A detailed description of the insulation vacuum for the cryomagnets can be found in reference [5].

2 SYNCHROTRON RADIATION

Synchrotron radiation in LHC is a dominant factor for the design of the vacuum system. At 7 TeV, the critical energy of the synchrotron radiation spectrum is 44 eV and the radiated power represents a heat load of 0.2 W/m per beam. To prevent this heat load reaching the 1.9 K cryogenic system, it has been proposed, since the early design phase, to install inside the cold-bore a 'beam screen' which can be operated at a temperature in the range of 5 to 20 K. However, the additional advantage of this beam screen is that it intercepts not only the synchrotron radiation, but removes also the resistive losses dissipated by the beam induced wall currents which are of comparable magnitude. The beam screen can also remove the more recently identified heat source by photoelectrons [6]. In the course of the experiments which were started for the SSC Project to study in detail the synchrotron radiation induced gas desorption in a cold vacuum system, it became evident that in the LHC, this screen had to be partially transparent so that H_2 molecules desorbed by the beam could be pumped permanently on the 1.9 K cold bore surface. Figure 1 shows a section of the circular cold-bore vacuum chamber (49 mm I.D.) and of the perforated beam screen, which has a carefully optimised section for both the horizontal (44 mm) and vertical (36 mm) apertures. Also shown in the figure are the pumping holes which represent approximately 4% of the surface. A more detailed discussion of the function of these pumping holes will be given later.
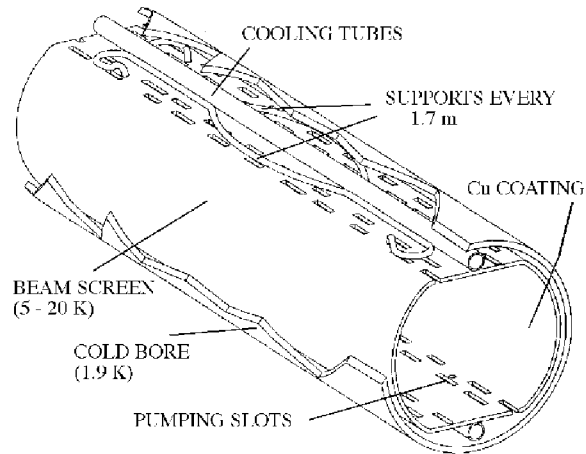

Figure: 1 Beam screen installed in the magnet cold-bore. Cooling pipes and supports are located in the vertical plane above and below the beam where the resulting aperture reduction can be accepted.

The beam screen is held in position with respect to the cold-bore by regularly spaced supports and cooled by two longitudinal helium pipes placed in the vertical plane above and below the beam. For mechanical and magnetic

reasons, the screen will be made of a low permeability stainless steel, approximately 1 mm thick. A detailed description of the required electric, magnetic and mechanical characteristics of the beam screen has been presented previously [7] and the most recent developments are presented in a separate contribution [8]. The inner wall, exposed to the electric field of the beam, will be coated with a 0.05 mm layer of high conductivity copper to keep the electric impedance low [9]. With this mechanical design of the beam screen an optimum compromise has to be found between several conflicting requirements. For example, the good electric conductivity of the copper conflicts with the magnetic forces produced by eddy currents during a magnet quench. These forces have been evaluated at several tons per m and impose the mechanically strong structure of the screen.

3 DYNAMIC VACUUM

The synchrotron radiation which strikes the inner copper coated surface of the beam screen is expected to produce a significant amount of desorbed gas in spite of the relatively low critical energy photon spectrum when compared with conventional synchrotron light sources. The linear photon flux (photons s^{-1} m^{-1}) depends on the beam current I(A) and the beam energy E(TeV) and the bending radius, in LHC it is given by 2.5×10^{16} I E . It is interesting to note that LHC will have a larger linear photon flux then LEP2 or the SSC. The resulting flow of photo-desorbed gas is proportional to the photon flux and to the molecular desorption yield. Over the last years, an intensive program of measurements has been undertaken, using mainly an external photon beam line on the EPA storage ring in CERN to obtain reliable data for the molecular desorption yields for representative vacuum chamber surfaces at the relevant photon energies and covering the temperature range from room temperature to 4.2 K [10], as shown in Table 1.

Table 1
Molecular desorption yield (molecules/photon) for copper plated stainless steel and for 45.3 eV critical energy photon spectrum at perpendicular photon incidence. From reference [10].

T (K)	H_2	CH_4	CO	CO_2
300	$5.0 \ 10^{-4}$	$1.6 \ 10^{-3}$	$2.5 \ 10^{-4}$	$2.2 \ 10^{-4}$
77	$2.5 \ 10^{-4}$	$4.0 \ 10^{-6}$	$1.5 \ 10^{-5}$	$7.0 \ 10^{-6}$
4.2	$3.5 \ 10^{-5}$	$8.0 \ 10^{-7}$	$6.0 \ 10^{-6}$	$7.0 \ 10^{-6}$

These latest results indicate a decrease of the molecular desorption yield with temperature but at 4.2 K, the observed yields are still significant. In addition, the effect of the grazing photon incidence in LHC has yet to be included. This dependence on photon incidence has been studied by measurements on a photon beam line at the VEPP-2M storage ring at INP in Novosibirsk [11]. There it was found that the molecular desorption yield for H_2 from a copper coated surface at about 10 K and under grazing incidence (~10 mrad) is approximately 5.10^{-4} molecules per photon (measured after an initial exposure to a photon dose of $2 \ 10^{21}$ photons/m), hence a factor of 14 larger than the corresponding value in Table 1.

4 NUCLEAR SCATTERING

Beam loss due to nuclear scattering on the residual gas represents a non-negligible heat load in LHC. Since these losses are due to interaction of high energy protons with the residual gas, the secondaries are sufficiently energetic to escape from the vacuum chamber and deposit their energy in the cryomagnets. There are two limits to the residual gas density, the first due to a concentrated, local heat load which could quench a magnet and the second from the distributed, total load to the cryosystem. The first limit applies to a local region with a high pressure (e.g. as it could be caused by a helium leak) while the second can be expressed in terms of the average gas density around the machine or more conveniently by the nuclear scattering beam lifetime τ(h).

P_{ns} (W/m) = 0.93 E(TeV) I(A)/τ(h).

The design of the LHC includes a nuclear scattering allowance of ~0.1 W/m for the two beams and this specifies a lower limit for the beam-gas lifetime of 69 hours; thus a 'lifetime limit' of 100 hours has been chosen to design the vacuum system. The local 'quench limit' on gas density, depending on the efficiency of the collimation system, is expected to be at least a factor 100 higher.

Gas densities are related to beam lifetime τ through the relation $1/\tau = \sigma$ c n , where σ is the total nuclear scattering cross section at 7 TeV, n the gas density and c the velocity of light. For H_2 and for the other molecular species in the residual gas Table 2 gives the relative nuclear scattering cross sections with respect to H_2 and the densities (m^{-3}) corresponding to a100 h beam life time.

Table 2
Relative nuclear scattering cross sections with respect to H_2 and densities corresponding to a100 h beam life time in LHC

Molecules	σ_i/σ_{H2}	n (m^{-3}) τ=100h
H_2	1	$9.8 \ 10^{14}$
He	1.26	$7.7 \ 10^{14}$
CH_4	5.4	$1.8 \ 10^{14}$
H_2O	5.4	$1.8 \ 10^{14}$
CO	7.8	$1.2 \ 10^{14}$
CO_2	12.2	$3.0 \ 10^{14}$

The 100 h beam lifetime limit requires an equivalent H_2 density $< 10^{15}$ m^{-3}. At the temperature of the beam screen (average ~10 K), this corresponds to 10^{-9} Torr.

5 BEAM INDUCED HEAT LOAD

The justification for a beam screen to intercept the power from the various beam related sources which otherwise would reach the cold bore and load the 1.9 K cryogenic system can be seen in Figure 2. Apart from the resistive losses in the beam screen all other heat loads increase with the beam energy. The contribution from photoelectrons will be discussed in a subsequent section.
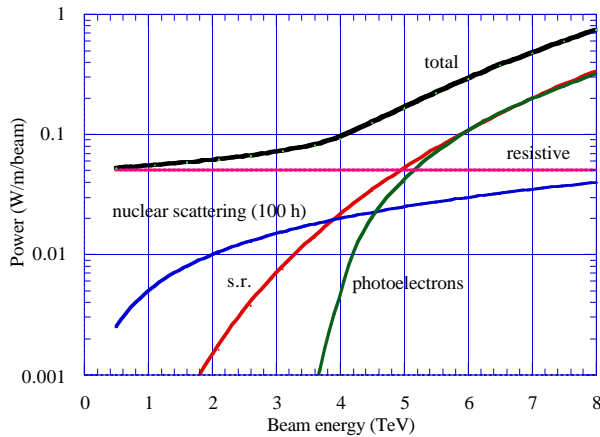

Figure: 2 Estimated and assumed beam induced losses in LHC. The contribution from photoelectrons will be discussed in a later section. Nuclear scattering is the only part which can not be removed by the beam screen.

6 VAPOUR PRESSURE

The cold length of the LHC vacuum system (some 80% of the circumference) relies on the cryopumping of the 1.9 K vacuum chamber through the perforated beam screen. Among the desorbed gases, hydrogen, which has the largest molecular desorption yield, is the most critical species for which the vapour pressure is high and the pumping capacity of the beam screen, operated between 5 and 20 K, is very small. Without the pumping holes, the cryopumping of the beam screen would not provide any useful capacity for LHC operation. In fact, the equilibrium vapour density at 5 K for a monolayer of hydrogen exceeds by several orders of magnitude the acceptable limit [12]. With the concept of pumping holes in the beam screen, hydrogen, and even more so all other gas species, can be pumped on the 1.9 K surface with a negligibly low saturated vapour density and hence in practical an unlimited capacity. Effectively, the pumping holes provide a constant pumping speed, proportional to the surface area of the holes and which can be optimised for different requirements. However, one important exception is He since even at 1.9 K, only a small amount of this gas can be accommodated and this highlights the importance of a perfect leak tightness for the beam vacuum system.

7 RECYLING OF PHYSISORBED GAS

Due to the photon flux which strikes the inner surface of the beam screen, cryopumped gas molecules on the screen may be re-desorbed. Measurements of this 'recycling' coefficient (secondary desorption) for hydrogen [13] give values increasing in proportion to the surface coverage and reaching approximately 1 molecule per photon at a monolayer. For any significant molecular coverage of the beam screen, this secondary effect for H_2 is several orders of magnitude larger than the primary desorption. The global result of thermal desorption and recycling will be that a limited equilibrium quantity of gas can be accommodated on the inner surface of the beam screen. Thereafter all the primary desorbed gas load will be transferred through the pumping holes to the 1.9 K vacuum chamber wall with a pumping speed now determined by the total hole area. A schematic picture of this process is illustrated in Figure 3.

The recycling coefficients for the important heavier gases, CH_4, CO and CO_2 have also been measured and it was found that even for thick physisorbed layers (10-20 monolayers) these coefficients are small and can not be distinguished from the respective primary photodesorption coefficients [14] i.e., they range below 10^{-3} molecules/photon. Fore these gases the recycling will be small and the pumping speed will remain, in contrast to H_2, at the level determined by the screen area and the respective sticking coefficient.

This behaviour of the vacuum system is illustrated in Figure 4 which shows experimental results from a prototype beam screen at the VEPP-2M photon beam line. The data have been scaled to the photon flux in the LHC at 1/10 of the nominal current. With a ~2% area of pumping holes, hydrogen saturates at ~3 10^{13} m^{-3}, well below the specified lifetime limit.

An important parameter for the design of the LHC vacuum system is also the total amount of desorbed H_2. This quantity has been estimated as 2.6 monolayers during the initial year of operation and as 10.5 monolayers during the second year at the full nominal beam current. This large quantity of gas should not pose a problem with the present design of the LHC vacuum system since the molecules can diffuse through the pumping holes and be adsorbed on the 1.9 K cold bore with a negligible vapour pressure.
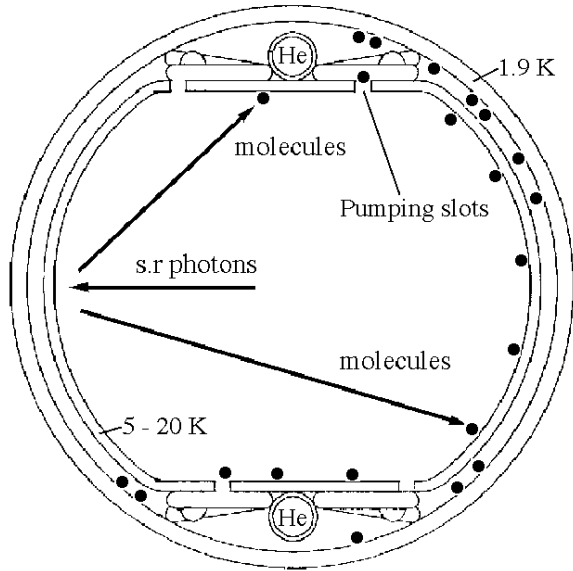
Figure: 3 Beam screen function with primary desorption and recycling of physisorbed gas. Permanent adsorption occurs on the 1.9 K cold-bore surface, protected by the beam screen from synchrotron radiation and photoelectrons.
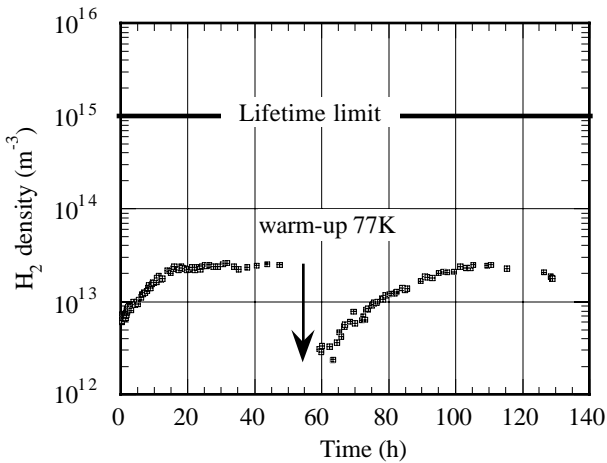

Figure: 4 Evolution of the molecular density of H_2 during photon exposure in an experiment at VEPP-2M with a perforated beam screen to simulate LHC during the first running year with 1/10 of the nominal beam current. During the experiment, the screen has been warmed-up to 77 K, while maintaining the cold-bore at ~3K, to the remove cryosorbed hydrogen and thus to demonstrate the repetition of the recycling effect.

8 ION INDUCED PRESSURE INSTABILITY

In the LHC, the ionisation of the residual gas molecules will produce ions which then are repelled by the positive beam potential and accelerated towards the beam screen or the vacuum chamber wall. The final energy of the ions may be up to 300 eV. As for the photons, the energetic ions can desorb tightly bound gas molecules with a molecular desorption yield, η_i (molecules per ion). Desorbed molecules will in turn be ionised and participate in the desorption process. This positive feedback can lead to the so-called 'ion induced pressure instability' known from previous experience with the Intersecting Storage Rings (ISR) at CERN. The pressure runaway depends critically on the local cleanliness of the surface, via the ion induced molecular desorption yield, and on the local pumping speed. The stability limit is expressed by the condition that the product of beam current I and of the molecular desorption yield η_i must be less than a limit given by the pumping speed

$$\eta_i \, I < \frac{e}{\sigma} \, S_{eff}$$

where e is the electron charge, σ the ionisation cross section of the residual gas molecules for high energy protons (typically 20 barn for hydrogen) and S_{eff} is the effective linear pumping speed. In the cold sections of the LHC, a well defined, lower limit of the pumping is determined by the cryosorption on the 1.9 K vacuum chamber surface through the pumping holes. The safe condition for vacuum stability for the cold sections is defined by the area A_f of pumping holes per unit length

$$\eta_i \, I \, < \, \sqrt{\frac{kT}{2\pi m}} \, \frac{e}{\sigma} A_f$$

with k the Boltzmann constant and m the mass of the molecules.

With the parameters of LHC, the stability limit for hydrogen is $\eta_i \, I = 10^3$ A. Since a typical primary ion desorption yield for an unbaked surface is of order unity, and since the large recycling coefficient for hydrogen does not permit the formation of a thick layer of H_2 on the screen, the cold sections of LHC will operate well inside this stability limit. However, this situation will be different in the room temperature sections, where the conventional, external pumping system is limited through the conductance of the beam pipe. The control of the η-parameter by appropriate surface preparation and by bakeout will be essential.

9 PHOTOELECTRONS AND MULTIPACTING

Beam induced multipacting [15] which may arise through synchronous motion of photoelectrons and low energy secondary electrons bouncing back and forth between opposite vacuum chamber walls with successive proton bunches represent a potential problem for the machine [16]. In the LHC the beam screen radius $r_p = 22$ mm, the bunch intensity $N_b = 1 \, 10^{11}$ protons and the bunch spacing $L_{bb} = 7.5$m are such that the wall-to-wall multipacting threshold, given by

$$N_b = \frac{r_p^2}{r_e \, L_{bb}} \quad , \; (r_e \text{ the classical electron radius}),$$

can be reached at about 1/4 only of the nominal intensity [6].

An additional effect attributed to synchrotron radiation is the production of photoelectrons a source which largely dominates electrons from residual gas ionisation. Measurements on the photon beam line at EPA [17] with an LHC test chamber give a photo-yield of typically 0.02 electrons/photon for the synchrotron radiation spectrum in LHC. Due to the strong electric field of the proton bunches these electrons can be accelerated across the beam pipe and transfer energy to the beam screen. A first, still very approximate estimate of this effect gives 0.2 W/m [6]. An additional consequence of these photoelectrons will be enhanced outgassing which will add to the photo-desorption.

10 MECHANICAL DESIGN

The mechanical design of the cold arc vacuum system requires a large number of interconnections for the beam vacuum between the beam screens of adjacent magnets. Following the proven design of the LEP-type RF-finger contacts a new concept has been developed which takes into account the large thermal contraction (approx. 45 mm) between room temperature and operating temperature. An important design criterion to be met is the requirement of installation and alignment of the long cryomagnets without the risk of damaging the delicate finger contacts. The principle of the proposed novel solution is shown in Figure 5 where the R.T. and the cold positions of the RF-bridge are drawn on the lower and on the upper section respectively18 [18].
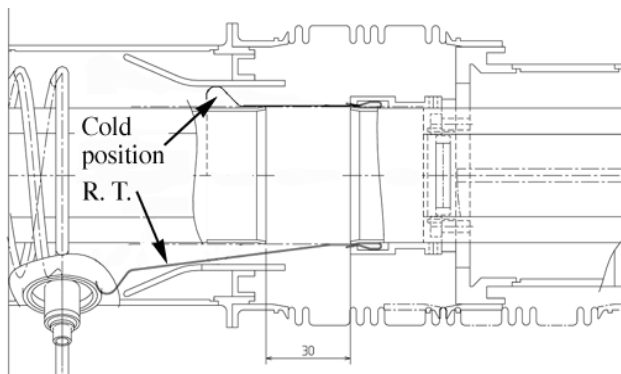

Figure: 5 Beam vacuum interconnection between magnets with a novel RF-bridge design to guarantee flexibility during installation and alignment. Lower section shows room temperature (R.T.) position, upper section shows the contact position at cryogenic temperature.

Only once the final cold position is reached, will the required smooth and well defined electric contact be established with a controlled contact force.

11 ACKNOWLEDGEMENTS

12 REFERENCES

[1] CERN/AC/95-05 (LHC), 20 October 1993.
[2] Mathewson, et al., EPAC 94, London, June 1994.
[3] Mathewson, et al., PAC 95, Dallas, 1995.
[4] Gröbner, Vacuum, 46, 767 (1995).
[5] Cruikshank, G. Engelmann, W. Koelemeijer, N.Kos, A.G. Mathewson, 5th European Vacuum Conference, Salamanca, 23-27 September, 1996.
[6] Gröbner, contribution to this conference.
[7] Poncet et. al., EPAC 94, London, June 1994.
[8] Cruikshank, et al., contribution to this conference.
[9] Ruggiero, R. Caspers, M. Morvillo, contribution to this conference.
[10] Vincent Baglin, Doctoral thesis, Université Denis Diderot Paris 7, UFR de Physique, Paris, May 1997.
[11] Calder, O. Gröbner, A.G. Mathewson, V.V. Anashin, A. Dranichnikov, O.B. Malyshev, J. Vac. Sci. Technol. A 14(4), Jul/Aug 1996.
[12] Wallén, J. Vac. Sci. Technol. A 15(2), March/April 1997.
[13] Anashin, O. Malyshev, V. Osipov, I. Maslennikov, W.C. Turner, 40th National Symposium AVS, Orlando, November 1993.
[14] Calder, O. Gröbner, A.G. Mathewson, V.V. Anashin, O.B. Malyshev, 5th European Vacuum Conference, Salamanca, 23-27 September, 1996.
[15] Gröbner, 10th Int. Conf. on High Energy Accelerators, Protvino, July 1977.
[16] Zimmermann, LHC Project Report 95, 27 February 1997.
[17] Goméz-Goñi, O. Gröbner, A.G. Mathewson, J.Vac.Sci. Technol. A 12(4), July/August 1994.
[18] Brunet, P. Cruikshank, P. Lepeule, I. Nikitine, C. Reymermier, G. Schneider, R. Veness, unpublished, April, 1997.